



SURFACE EFFECTS OF PLATINUM NANOWIRE UNDER UNIAXIAL TENSILE LOADING: A MOLECULAR DYNAMICS SIMULATION STUDY

Vildan Guder*

Department of Physics, Faculty of Science, Trakya University, Edirne, Turkey

ARTICLE INFO

Article history:

Received 30 September 2021

Accepted 6 December 2021

Keywords:

tensile, nanowire, Molecular Dynamics Simulation

ABSTRACT

The mechanism of the tensile deformation of face centered cubic platinum nanowires was investigated by molecular dynamics simulation in which the interactions are expressed by the embedded atom method potential. The two different thicknesses (1.9 nm and 9.8 nm) of nanowires were used to understand the role of surface effects on the mechanical properties of platinum nanowires. The yield stress and strain values were determined by the elastic recovery test which was performed for both nanowires. For 9.8 nm platinum nanowire, the average stress has been governed by core atoms while the surface atoms are more effective to define the mechanical properties of the 1.9 nm platinum nanowire.

© 2021 Journal of the Technical University of Gabrovo. All rights reserved.

INTRODUCTION

Metallic nanowires (NW) have numerous applications in many different fields, such as nanoscale wiring of integrated circuits [1], used for catalysis, as a superconductor and as nanopipette probes [2], and optoelectronic applications [3]. Various studies have been carried out for the fabrication, experimentation and simulation of metallic NWs and to determine the mechanical properties of metallic NWs. The mechanical failure and nano elastic processes observed during the fabrication of gold NWs were examined by molecular dynamics simulations (MD), and it was found that the local atomic order affects the hardness of gold NW [4]. Lucas et al. [5] investigated the plastic deformation of a pentagonal silver NW using atomic force microscopy (AFM) and observed a neck, surface atomic steps, nucleation of dislocations, and yielding. They reported the maximum stress to be 2 GPa. Jing et al. [6] observed a relation between Young's modulus and size for silver NW, which attributed to the oxidation layer and surface roughness. The Young's modulus, yield and fracture strength were calculated for nickel NWs at different strain rates and it was found that these calculated properties exhibit a linear relation according to the logarithm of the strain rate [7]. Guder and Sengul [8] revealed the relation between strain rate, temperature and size with the mechanical properties of zirconium NWs. Sengul et al. [9] have observed that the average stress of rhodium NWs thinner than the size of 2.8 nm is governed by the surface atoms. Platinum (Pt) NWs have recently considerable importance in applications in molecular electronics [10], nano actuators and very-high-frequency nanoelectromechanical systems [11]. Although many researchers have focused on gold, silver, and nickel

NWs, studies for Pt NWs are limited [12,13]. The surface effects on the mechanical properties of Pt NWs have not been studied. This study examines the stress-strain behavior of 1.9 nm and 9.8 nm Pt NWs and determines whether the mechanical responses of both nanowires are characterized by core or surface atoms.

EXPOSITION

A Large – scale Atomic-Molecular Massively Parallel Simulator (LAMMPS) served as an open-source code [14] was used to investigate the surface effects of Pt NWs during tensile process. The interactions between Pt atoms were expressed by the embedded atom method potential (EAM) developed and reparametrized by Sheng [15]. The initial configuration of simulations was the ideal face centered cubic (fcc) lattice. The bulk system was energy-minimized by using the conjugate gradient algorithm and the lattice constant and cohesive energy values were calculated. Table 1 lists the calculated physical values with the experimental data. It is seen that the results agree with experimental values.

Table 1 The calculated lattice constant and cohesive energy values for Pt.

	<i>This work</i>	<i>Exp.</i>
a (Å)	3.90	3.92 ^a
E (eV/atom)	-5.77	-5.77 ^a

^a[15]

The NW systems were formed by repeating the fcc unit cell in the x [100], y [010] and z [001] directions. We

* Corresponding author. E-mail: vildanguder@hotmail.com

formed two NWs of cross-sectional sizes of 1.9 and 9.8 nm with the same length (19.6 nm) where the multiplying factors are 5x5x50 (5000 atoms), 25x25x50 (125000 atoms), respectively. The tensile loading was applied along the z-direction. While the x and y axes were kept free, the periodic boundary conditions were applied along the z-axis. Fig. 1 show the top and side view of NW model systems. The atoms at both ends (blue spheres) at positions corresponding to 20% of the NW length were rigid, but other atoms (red spheres) were free to interact with each other. The shell at a thickness of 0.4 nm was selected from the outermost surface of the NW, and the atoms inside this shell were labelled as surface atoms and other atoms except for rigid atoms as core atoms. The model NW is shown in Figs. 1 (a, e) in top and side views consisted of two kind of atoms, free and rigid. Figs. 1 (b, f) shows the NW system except for the rigid atoms that allow for free contraction or expansion on the side surfaces. We separate the free atoms in the middle region into two groups to investigate the surface effect on the mechanical properties of Pt NW. These two groups represent NW systems consisting of surface and core atoms in Figs. 1. (c, g) and Figs. 1. (d, h), respectively.

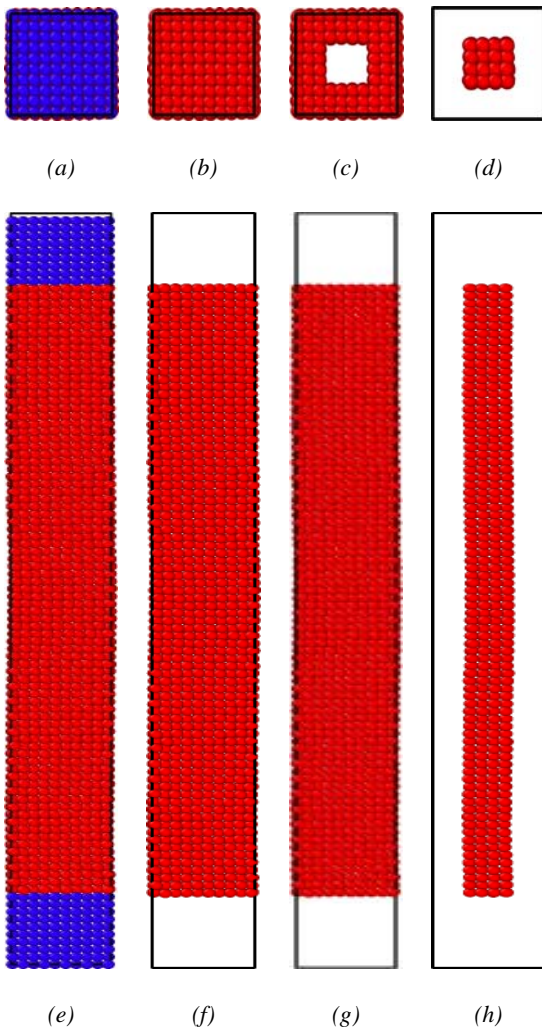


Fig. 1. Atomistic model for Pt NWs. The top view of (a) all (b) middle (c) surface (d) core and the side view of (e) all (f) middle (g) surface (h) core. The blue and red spheres represent rigid and free atoms.

Before tensile loading, NWs were relaxed within the microcanonical ensemble (NVE) at 300 K with 10000 MD steps and a time step of 0.001 ps. The isochoric and isothermal ensemble (NVT) and Nose-Hoover thermostat were used to simulate the tensile process of NWs. The 100% tensile load was applied to the NWs at a strain rate of 0.001 ps⁻¹. The total stress tensor was obtained from the virials for each atom as [16, 17].

$$\sigma_{tot}^{\alpha\beta} = \frac{1}{V_{tot}} \sum_{i=1}^N \left(-m_i v_i^\alpha v_i^\beta + \frac{1}{2} \sum_{j \neq i}^N F_{ij}^\alpha r_{ij}^\beta \right) \quad (1)$$

where α and β denote the components of Cartesian coordinates, V_{tot} is the volume of the system, m_i and v_i are the mass and velocity components of atom i , F_{ij} is the force on atom i exerted by atom j and r_{ij} is the distance between atoms i and j . To express the total (average) stress in terms of surface and core stress, Equation 1 is given as [18]:

$$\sigma_{tot}^{\alpha\beta} = \frac{V_{surf}}{V_{tot}} \sigma_{surf}^{\alpha\beta} + \frac{V_{core}}{V_{tot}} \sigma_{core}^{\alpha\beta} \quad (2)$$

where the $\sigma_{surf}^{\alpha\beta}$ and $\sigma_{core}^{\alpha\beta}$ represent the surface and core stresses, V_{surf} and V_{core} denote the volumes for relevant regions. The strain-dependent variations of stress for 1.9 nm and 9.8 nm Pt NWs at the temperature of 300 K have been depicted in Fig. 2 and Fig. 3, respectively. Additionally, they show the effect of core and surface atoms on the overall stress of Pt NWs. The curves can be separated into two parts: elastic (I) and plastic (II) regions. In region I., the stress changes linear with increasing strain. The bonds between atoms lengthen with tensile, when the tension is removed, the bonds shorten homogeneously and the system returns to its initial form. The yield stress and strain which define the limit of the region I, were determined by the elastic recovery test which was performed for both NWs. The yield stress corresponds to the value of maximum stress. To illustrate elastic recovery, the change in volume as a function of MD simulation time for different strains for 1.9 nm and 9.8 nm Pt NWs is given in Fig. 4 and Fig. 5, respectively. When the load is removed at strains of 0.075 and 0.089 (elastic limits), the systems are observed to recover themselves for 1.9 nm and 9.8 nm Pt NWs, respectively. When the tension is removed at the yield strains (stresses) of 0.076 (13.9 GPa) and 0.090 (12.2 GPa), atoms leave regular lattice points for 1.9 nm and 9.8 nm Pt NWs, respectively. In region II which begins sharp drop in stress, the system cannot return to its original state. In this case, the plastic deformation which is irreversible permanent is observed due to the deformation on the surface of the NW [19]. With the increase of plastic deformation, the cross-sectional area of NW narrows at relevant region and a neck (irregular shape) is formed at strain values of 0.079 and 0.110 for 1.9 nm and 9.8 nm NWs, respectively. Then, the stress approaches zero with increasing/decreasing cyclic change and drops to zero at the 18.7% and 71.5% strains, which reflects the separating of Pt NWs into two small clusters for 1.9 nm and 9.8 nm, respectively. In Fig. 2 and Fig. 3, the stress of atoms in the thickness of 0.4 nm regions from the surface of the NWs is labelled "surface stress", and the stress of all atoms in the systems except for shell and rigid atoms is labelled "core

stress". The "NW" term represents the overall stress of systems, except for rigid atoms. The surface and core stress has similar stress-strain behavior as NW. But, for 9.8 nm Pt NW, the average stress has been governed by core atoms while the surface atoms are more effective to define the mechanical properties of 1.9 nm Pt NW.

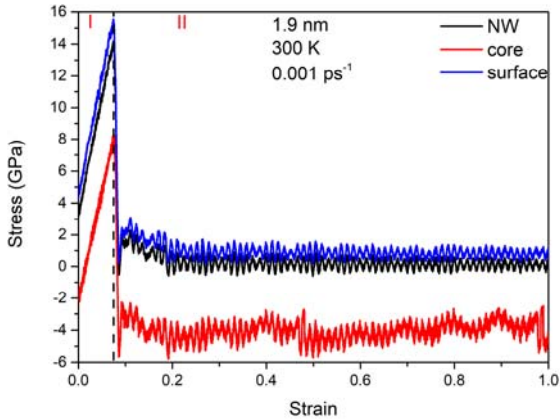


Fig. 2. The stresses for the surface, core and entire system except for rigid atoms for 1.9 nm Pt NW

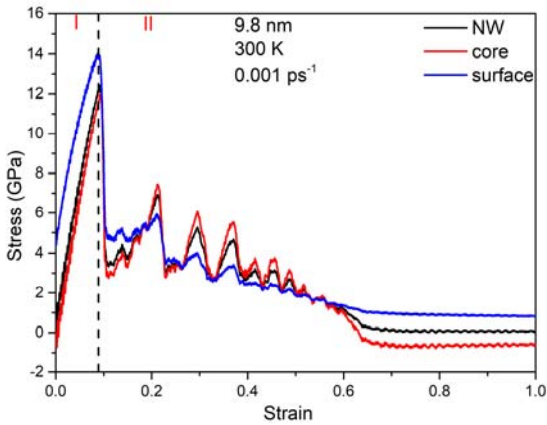


Fig. 3. The stresses for the surface, core and entire system except for rigid atoms for 9.8 nm Pt NW

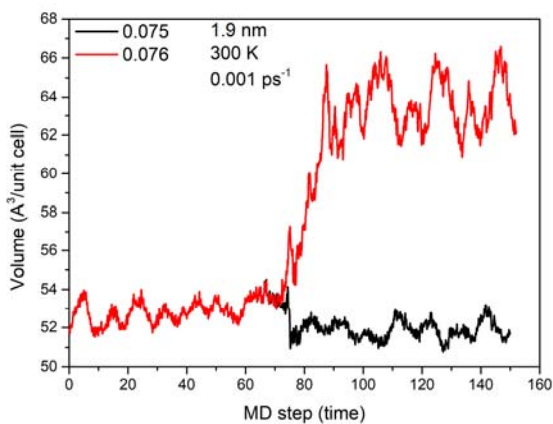


Fig. 4. The elastic recovering process of 1.9 nm Pt NW when the load removed at yield strain (red line) and elastic strain (black line)

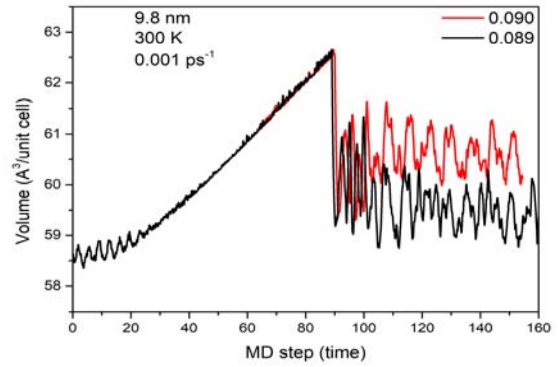


Fig. 5. The elastic recovering process of 9.8 nm Pt NW when the load removed at yield strain (red line) and elastic strain (black line)

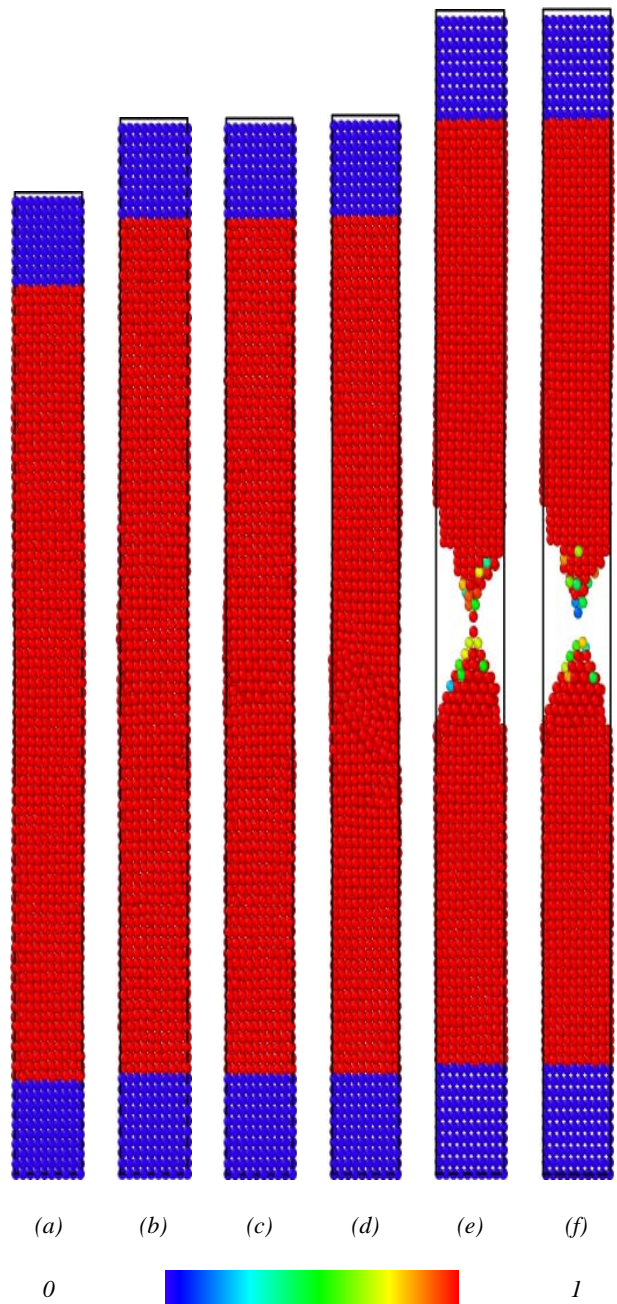


Fig. 6. MD simulation snapshots at the strains of (a) 0, (b) 0.075, (c) 0.076, (d) 0.079, (e) 0.186 and (f) 0.187 for 1.9 nm NW. The atoms are colored according to von Mises stress.

The shape change (local shear) during tensile loading can be presented by von Mises stress [20]. For an atom i , it is given by

$$\eta_i = \sqrt{0.5 \left[(\sigma^{xx} - \sigma^{yy})^2 + (\sigma^{yy} - \sigma^{zz})^2 + (\sigma^{zz} - \sigma^{xx})^2 + 6 \left((\sigma^{xy})^2 + (\sigma^{yx})^2 + (\sigma^{xz})^2 \right) \right]} \quad (3)$$

Fig. 6 represent MD simulations images taken at (a) initial, (b) elastic limit, (c) yield strain, (d) neck strain, (e) before fracture strain and (f) fracture strain during tensile loading for 1.9 nm NW, respectively. Fig. 6 (a) displays that the initial system without load. With increasing strain, the deformation develops homogeneously in the system (Fig. 6(b)) and then plastic deformation occurs (Fig. 6(c)). The neck formation and slip plane are observed in Fig. 6(d). In Fig. 6 (e) shows small Pt chain before fracture of NW. In Fig. 6(f), it is seen that the NW system is broken into two separate clusters.

CONCLUSION

The mechanism of the tensile deformation of fcc Pt NWs has been investigated by MD simulation using the EAM potential. The two different thicknesses (1.9 nm and 9.8 nm) of NWs have been used to understand the role of surface effects on the mechanical properties of Pt NWs. The elastic limits were determined at the strain of 0.075 and 0.089 for 1.9 nm and 9.8 nm Pt NW, respectively. The irreversible permanent plastic deformation occurs at yield strains (stresses) of 0.076 (13.9 GPa) and 0.090 (12.2 GPa) for 1.9 nm and 9.8 nm Pt NWs and the atoms leave regular lattice points. With the increase of plastic deformation, the cross-sectional area of NW narrows at relevant region and a neck (irregular shape) is formed at strain values of 0.079 and 0.110 for 1.9 nm and 9.8 nm NWs, respectively. Further increasing the load, Pt NWs break into two small clusters at the strains of 18.7% and 71.5% for the thickness of 1.9 nm and 9.8 nm, respectively. The surface and core stress has similar stress-strain behavior as NW stress. But, for 9.8 nm Pt NW, the average stress has been governed by core atoms while the surface atoms are more effective to define the mechanical properties of the 1.9 nm Pt NW.

REFERENCES

- [1] Dubois S., Piraux L., George J.M., Ounadjela K., Duvail J.L., Fert A. Evidence for a short spin diffusion length in permalloy from the giant magnetoresistance of multilayered nanowires. *Phys Rev B - Condens Matter Mater Phys.* 1999
- [2] Shao Y., Mirkin M.V., Fish G., Kokotov S., Palanker D., Lewis A. Nanometer-Sized Electrochemical Sensors. *Anal Chem [Internet].* 1997 Apr 1;69(8):1627–34. Available from: <https://pubs.acs.org/doi/10.1021/ac960887a>
- [3] Christ A., Zentgraf T., Kuhl J., Tikhodeev S.G., Gippius N.A., Giessen H. Optical properties of planar metallic photonic crystal structures: Experiment and theory. *Phys Rev B [Internet]* 2004 Sep 28 70(12):125113. Available from: <https://link.aps.org/doi/10.1103/PhysRevB.70.125113>
- [4] Rubio-Bollinger G., Bahn S.R., Agraït N., Jacobsen K.W., Vieira S. Mechanical Properties and Formation Mechanisms of a Wire of Single Gold Atoms. *Phys Rev Lett* 2001 Jun 20;87(2):026101. Available from: <https://link.aps.org/doi/10.1103/PhysRevLett.87.026101>
- [5] Lucas M., Leach A.M., McDowell M.T., Hunyadi S.E., Gall K., Murphy C.J. et al. Plastic deformation of pentagonal silver nanowires: Comparison between AFM nanoindentation and atomistic simulations. *Phys Rev B.* 2008 Jun 77(24):245420
- [6] Jing G.Y., Duan H.L., Sun X.M., Zhang Z.S., Xu J, Li Y.D. et al. Surface effects on elastic properties of silver nanowires: Contact atomic-force microscopy. *Phys Rev B* 2006 Jun 13 73(23) 235409 Available from: <https://link.aps.org/doi/10.1103/PhysRevB.73.235409>
- [7] Huang D., Zhang Q., Qiao P. Molecular dynamics evaluation of strain rate and size effects on mechanical properties of FCC nickel nanowires. *Comput Mater Sci* 2011 Jan 50(3):903–10 Available from: <https://linkinghub.elsevier.com/retrieve/pii/S0927025610005872>
- [8] Guder V., Sengul S. Tensile strength and failure mechanism of hcp zirconium nanowires: Effect of diameter, temperature and strain rate. *Comput Mater Sci.* 2020 May 177:109551
- [9] Sengul S., Guner A.K., Guder V. Surface effects on the mechanical properties of rhodium nanowires by molecular dynamics simulations. *Phys B Condens Matter* 2021 Dec 622:413344. Available from: <https://linkinghub.elsevier.com/retrieve/pii/S0921452621005123>
- [10] Smit R.H.M., Noat Y., Untiedt C., Lang N.D., van Hemert M.C., van Ruitenbeek J.M. Measurement of the conductance of a hydrogen molecule. *Nature* 2002 Oct 31 419(6910) 906–9. Available from: <http://www.nature.com/doi/10.1038/nature01103>
- [11] Husain A., Hone J., Postma H.W.C., Huang X.M.H., Drake T., Barbic M. et al. Nanowire-based very-high-frequency electromechanical resonator. *Appl Phys Lett* 2003 Aug 11 83(6):1240–2. Available from: <http://aip.scitation.org/doi/10.1063/1.1601311>
- [12] Cheng Q.H., Lu C., Lee H.P. A molecular dynamics simulation of hexagonal solid platinum nanowires. *Mol Simul* 2005 Apr 31(4) 289–93 Avail. from: www.tandfonline.com/doi/abs/10.1080/08927020412331333720
- [13] Koh S.J.A., Lee H.P., Lu C., Cheng Q.H. Molecular dynamics simulation of a solid platinum nanowire under uniaxial tensile strain: Temperature and strain-rate effects. *Phys Rev B* 2005 Aug 3 72(8):085414. Available from: <https://link.aps.org/doi/10.1103/PhysRevB.72.085414>
- [14] Plimpton S. Fast Parallel Algorithms for Short-Range Molecular Dynamics. *J Comput Phys* 1995 117(1) 1–19. Available from: <http://www.sciencedirect.com/science/article/pii/S002199918571039X>
- [15] Sheng H.W., Kramer M.J., Cadieu A., Fujita T., Chen M.W. Highly optimized embedded-atom-method potentials for fourteen fcc metals. *Phys Rev B.* 2011 Apr;83(13):134118
- [16] Rabkin E., Nam H-S., Srolovitz D.J. Atomistic simulation of the deformation of gold nanopillars. *Acta Mater* 2007 Apr 55(6) 2085–99 Available from: linkinghub.elsevier.com/retrieve/pii/S1359645406008202
- [17] Thompson A.P., Plimpton S.J., Mattson W. General formulation of pressure and stress tensor for arbitrary many-body interaction potentials under periodic boundary conditions. *J Chem Phys* 2009 Oct 21 131(15):154107. Available from: <http://aip.scitation.org/doi/10.1063/1.3245303>
- [18] Zhang Q., Li Q-K., Li M. Internal stress and its effect on mechanical strength of metallic glass nanowires. *Acta Mater* 2015 Jun 91:174–82 from: <https://linkinghub.elsevier.com/retrieve/pii/S1359645415001962>
- [19] Rabkin E., Srolovitz D.J. Onset of Plasticity in Gold Nanopillar Compression. *Nano Lett* 2007 Jan 7(1):101–7. Available from: <https://pubs.acs.org/doi/10.1021/nl0622350>
- [20] von Mises R. *Mechanik der festen Körper im plastisch-deformablen Zustand.* Nachrichten von der Gesellschaft der Wissenschaften zu Göttingen, Math Klasse. 1913